Interaction of a 24 GeV Proton Beam with a Muon Collider Mercury Jet Target. Experimental Results and Thermodynamic Assessment

N. Simos[1], H. Kirk[1], K. McDonald[2], C. Finfrock[1], G. Greene[1], H. Ludewig[1], P. Thieberger[1], and N. Mokhov[3]

[1]*Brookhaven National Laboratory, Upton, NY 11973, USA; simos@bnl.gov*
[2]*Princeton University, USA*
[3]*Fermi National Accelerator Laboratory, USA*

Abstract

A muon collider or a neutrino factory based on a muon storage ring require intense beams of muons that can be generated by a 1-4 MW proton beam incident on a moving target inside a 20-T solenoid magnet, with a mercury jet as a preferred example. This paper addresses the thermodynamic interaction of the intense proton beam with the proposed mercury jet target, and the consequences of the generated pressure waves on the target integrity. Specifically, a 24 GeV proton beam with approximately 16 TP (1 TP = 10^{12} protons) per pulse and a pulse length of 2 ns will interact with a 1 cm diameter mercury jet within the 20-Tesla magnetic field. In one option, a train of six such proton pulses is to be delivered on target within 2 μs, in which case the state of the mercury jet following the interaction with each pulse is critical. Using the equation of state for mercury from the SESAME library, in combination with the energy deposition rates calculated the by the hadron interaction code MARS, the induced 3-D pressure field in the target is estimated. The consequent pressure wave propagation and attenuation in the mercury jet is calculated using a transient analysis based on finite element modeling, and the state of the mercury jet at the time of arrival of the subsequent pulse is assessed. Issues associated with the use of a liquid metal jet as target candidate are addressed as compared to issues in solid targets. Lastly, some experimental results from the BNL E951 experiment are presented and discussed.

1. INTRODUCTION

In the conceptualized muon collider or neutrino factory a tightly focused, high intensity proton beam is required on a primary target. For the desired production of pions a 1-4 MW proton beam is envisioned impinging on a preferably high-Z target material within a 20-Tesla solenoid magnet. While a number of simulation studies have been performed on various solid and liquid targets for proton energies ranging between 8-30 GeV, the most favorable target appears to be a free mercury jet. Figure 1 depicts the pion production from a range of GeV protons on various target materials. It should be pointed out that key target parameter is its radius (important in the pion yield that is affected by re-absorption in the high-Z materials) which has been optimized in the study.
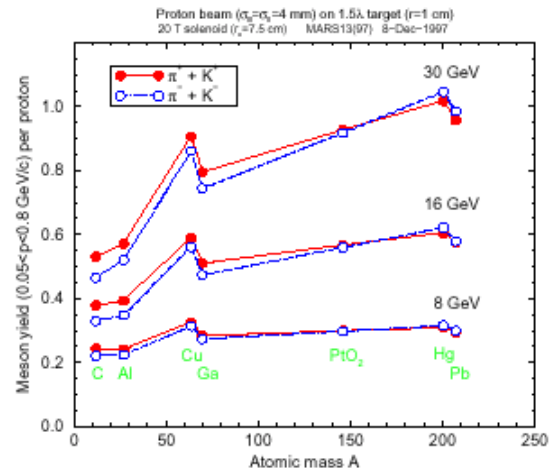
Figure 1: Pion production from different GeV protons in high and low-Z target materials

The use of a mercury jet target, however, raises several novel issues that need to be carefully examined. These include dispersion of the jet due to rapid energy deposition, destruction of the jet by magnetic forces, and ejection of high velocity droplets that can damage the confining envelope. Additionally, challenging design issue within the target space is the possibility of shock wave impact and consequently potential damage on the jet nozzle that sends the jet into the solenoid.

The proposed target is a 1cm diameter mercury jet ejected from a nozzle into a 20 Tesla magnetic field where it is intercepted by a 24 GeV, tightly focused proton beam with 0.5-1.5 mm rms sigma radius and intensity of 16 TP. One option that has been examined, and is the focus of this paper, is a train of six 2 ns long pulses on target.

Recently, a different proton beam structure on target has been studied in lieu of technical difficulties in achieving such fast delivery of beam. Both scenarios are discussed in this paper. For either scenario, however, the proton intensity of each of the six micro-pulses, combined with the short pulse length, is bound to induce very high pressures in the mercury. While the major

issue is the likelihood of jet destruction from a single micro-pulse, the potential for pressure waves arriving at the nozzle is of engineering importance. These pressure waves are generated in the Hg jet from its interaction with the proton beam and travel back toward the nozzle along the undisturbed jet.

Within the context of the BNL E951 experiment, a mercury jet and carbon targets have been exposed to 24 GeV protons of up to 4 TP per single bunch and focused down to 0.6 x 1.6 mm^2 spot. Dispersal of the mercury jet was observed with velocities up to 50 m/sec. Evidence of nozzle exposure to pressure waves was also recorded. A summary of the mercury jet experiment is included in a section of this paper.

2. MUON PRIMARY TARGET

Figure 2 is a schematic view of pion production, capture and initial phase rotation. As shown, a 24 GeV proton beam is incident on a skewed target inside the high-field solenoid magnet followed by a decay and phase rotation channel. The current (optimized for pion yield) tilted beam/jet configuration, shown in Figure 3, calls for a mercury jet at 100 mrad and the proton beam at 66 mrad. An additional consideration of any configuration is the need to have a sufficient interaction region (2-3 interaction lengths) something that favors a high-Z target material such as mercury given the geometrical constraints.
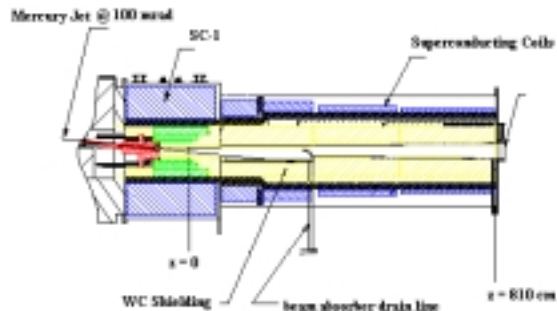
Figure 2: Schematic concept of targetry and capture based on a tilted configuration of proton beam and mercury jet.
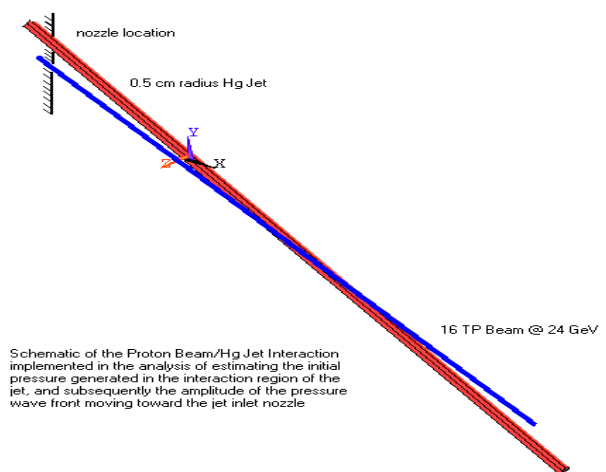
2.1 Mercury Jet Target Issues

The use of a mercury jet target raises a number of issues that need considerable attention. These issues are associated with the presence of a strong magnetic field, the rapid heating of the mercury by the proton beam and the subsequent dispersion.

As the mercury jet enters the field eddy currents are induced in the jet and the Lorentz force on these currents could lead to the distortion of the jet. The interaction of the mercury jet with the magnetic field is studied in detail in [5,6,7] with reference to experimental data. An important point to be made is the generated magnetic pressure on the mercury jet that is expected to damp mechanical perturbations and also add inward radial pressure.

Preliminary estimates (verified by the E951 experiment) have shown that the mercury jet will disperse after it interacts with a single proton pulse. What is key, however, is estimating the time scale of jet destruction. For this study that evaluates the scenario of six (6) 2-ns micro-pulses within 2 μs, the time of destruction is important in that the goal is to have all six micro-pulses see an intact jet. A consequence of the jet's dispersion is the ejection of droplets that, when at very high velocities, can cause serious damage to the target space.

Noted earlier is a concern related to the survivability of the jet nozzle experiencing a pressure wave effect that travels toward the nozzle. For a continuous jet with the interaction zone starting at some distance downstream of the nozzle, pressure waves are expected to travel through the undisturbed jet and reach the nozzle. While pressure amplitudes are expected to attenuate by the time the front reaches the nozzle, the many cycles over the life of the target enclosure could lead to nozzle fatigue failure. Within the scope of E951 experiment, an attempt was made to address the issue and preliminary results are shown in a later section of this paper.

Figure 3: Tilted configuration: Schematic of proton beam/mercury jet target

2.2 Muon Collider Beam Structure

The baseline beam structure for this study consists of a train of six micro-pulses that are delivered on target within two (2) microseconds. Each micro-pulse has length of 2 ns and the time interval between them is approximately 440 ns. According to this beam delivery scheme, the jet and the beam are assumed co-linear. The current option [1], however, envisions a tilted configuration and a delivery scheme in which the time interval between bunches of 20 ms. Table 1 below is a summary of the latest beam parameters.

Table 1: Muon Collider Parameters - Study II

Beam σ_r (mm)	1.5
Beam angle to magnet axis θ_p (mrad)	−67
Jet material	mercury
Velocity v_s (m/s)	30
Jet radius r_s (mm)	5
Jet angle to magnet axis θ_{Hg} (mrad)	−100
Crossing angle $\theta_{crossing}$ (mrad)	33
t between bunches (ms)	20
z_{nozzle} (cm)	−60

2.3 Energy Deposition

For all scenarios of beam delivery, the energy deposited in the mercury jet has been calculated using MARS [11]. In the co-linear interaction of proton beam and jet, peak energies of approximately 130 Joules/gm have been estimated. This peak energy is observed about 5 cm into the jet from the start of the interaction region. In the latest scheme, however, with the mercury jet tilted by 100 mrad and the proton beam by 67 mrad the peak energy deposition is approximately 49 Joules/g and it occurs about 25 cm downstream from the start of the interaction region. The significant reduction in energy deposited per micro-pulse will affect the condition of the jet between micro-pulses as well as its overall response to the train of six.

2.4 Thermodynamic Interaction

Upon jet/proton beam interaction, two processes are initiated, namely thermodynamic response and pressure wave initiation and propagation. Assuming that "thermalization" times are much smaller than acoustic diffusion times, the mercury jet will experience an almost instantaneous temperature increase followed by pressure waves and, at a slower pace, expansion of the heated mercury outward. First, the thermodynamic

processes that take place within the system during the six-bunch pulse train are examined.

Physical Properties of Mercury
Density: $\rho = 13.5$ x g/cm^3
Compressibility: $\kappa = 0.45$ x 10^{-10} m^2/N
Volumetric Thermal expansion: $\alpha_v = 18.1$ x 10^{-5} K^{-1}
Specific Heat: $c_v = 140$ J/Kg K
Velocity of Sound = 1300 m/s
Critical Point Temperature: $T_{cr} = 1593^\circ$ C
Critical Point Pressure: $P_{cr} = 185$ MPa

While the initial temperature and pressure can be estimated using the approximate formulae,
$$\Delta Q = c_v \, \Delta T$$
$$\Delta P = \alpha_v \, \Delta T / \kappa$$
thermodynamic processes that take place between pulses need the equation of state for mercury in order to be traced properly (two independent properties will define the exact state). The SESAME library [9] for mercury provides such a relationship and is used to better assess the pressure and temperature increases resulting from the series of micro-pulses.
When the jet enters the target space the mercury is in a compressed liquid state. The surface tension γ (450 dyn/cm for mercury) induces a pressure in the jet,

$$P_{initial} = 2\gamma/r = 1800 \text{ dyn/cm}^2$$

This pressure is higher than the saturation pressure at the temperature indicating the initial compressed liquid state. At the end of the first micro-pulse, the mercury has increased its pressure and temperature through a constant volume process. During this process all the energy deposited by the beam is converted into internal energy. From the thermodynamic stand point the key question to be answered is whether the mercury in any part of the interaction zone has entered the critical regime (both pressure and temperature above the critical values). Based on peak energy depositions per micro-pulse of 130 J/g, the increase in temperature is approximately 940° C and the peak pressure 3780 MPa. Clearly no mercury has entered the critical regime after a single micro-pulse and so the jet is still a highly compressed liquid.

During the time interval between micro-pulses (440 ns), an adiabatic expansion of the pressurized mercury (adiabatic because heat transfer is much too slow a process to take place at these small times) is taking place. This implies that the entropy in the mercury at the end of the first micro-pulse and the start of the second is constant. To exactly define the state of the mercury at the beginning of the second micro-pulse the specific volume or density needs to be defined. The volumetric change of the heated mercury is proportional to the stretching of material that occurs at the interface of two

distinct zones. To estimate the volumetric change, consider an infinitesimal volume of mercury d**V** experiencing a change of temperature **ΔT** and pressure **ΔP**. From the relations below the outward velocity **U**r as function of sound velocity **c** of material in the jet can be estimated along with the volumetric change.

$$K.E. = \tfrac{1}{2}\, \rho \; dV \; U_r^2 = \Delta P \; \delta(dV)$$
$$\Delta P \approx \alpha_v \, \Delta T / k$$
$$\alpha_v = (\partial V / \partial T)_P$$
$$\delta(dV) = \alpha_v \, dV \, \Delta T$$
$$U_r^2 / c^2 = 2 \, \alpha_v^2 \, \Delta T^2$$
$$U_r = \sqrt{2} \, [\alpha_v \, \Delta T] \, c$$

It is apparent from the above relations that the movement of bulk material as a result of thermal gradients is just a percentage of the velocity of sound that generated pressure waves travel. So, while the pressure field is experiencing the passage of the generated pressure waves (superimposed onto the thermodynamic pressure) the exchange of heat and bulk material movement is governed by much slower processes (pressure waves do not move mass around).

Using the constant entropy process and the final specific volume (expansion resulted during the 440 ns) based on the volumetric material expansion the state of the mercury just before the arrival of the second pulse is defined. From the SESAME table, it is estimated that the mercury has not crossed the saturation line and is still a compressed liquid but of much higher temperature and pressure than it has originally started. The two-step process (constant volume heat addition and adiabatic expansion) repeats upon the arrival of the second pulse in the train. While the pressure at the end of the second pulse exceeds P_{cr}, the peak temperature in the jet (T_{max} = 1716 K) is still below T_{cr}. Following the adiabatic expansion, mercury moves further away from the critical point. This implies that after two successive pulses the mercury is still a compressed liquid while the elapsed time is approximately 884 ns. Repeating the two-step process for the third pulse it is estimated that the part of the jet with peak energy deposition crosses the critical point. The subsequent behavior of the jet and the interaction between distinct zones within it is an on-going effort. In [4] consequences of exceeding a threshold are discussed. Given the uncertainties of such state and its consequences on the jet integrity, avoiding it altogether is a preferred option.

Based on the latest scenario of a tilted beam/jet configuration, the estimated peak energies deposited per pulse are below 50 J/g. While complete calculations for this latest profile are not yet available, there is strong indication that the jet could possibly survive all six pulses without entering the critical zone even if the entire train is delivered in 2 µs.

2.5 Predictions of Pressure Wave Generation

Using the energy deposition of the head-on interaction scenario with peak value 130 J/g and the equation of state for mercury from [9] an initial temperature and pressure distribution was assessed for the 30 cm long and 1 cm radius jet. The initial pressure distribution was incorporated into a finite element model using the ANSYS [13] code and the wave equation was solved through a transient analysis.
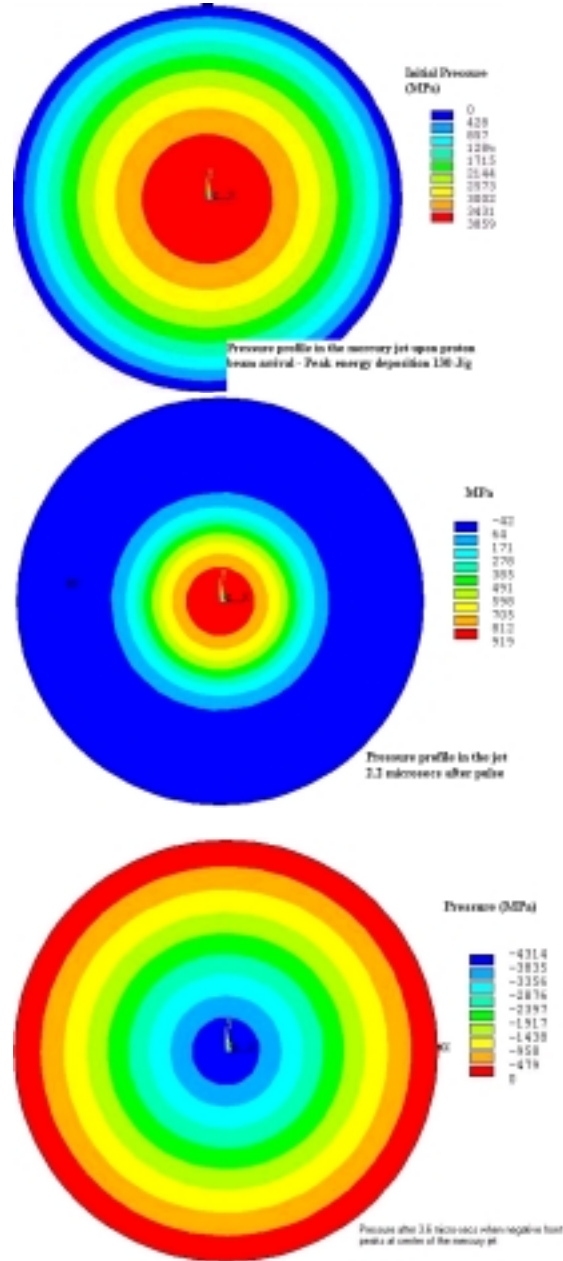
Figure 4: Pressure development in the cross section of the mercury jet with peak energy deposition

The primary goal of this analysis was to estimate the time scale in which high negative pressures start to appear in the jet. No further assessments, past the state of negative pressure, are attempted due to limitations of the computational tool. In conjunction with the previous section that deals with the thermodynamic processes that take place and the time structure of the pulse train, the time of high negative pressure generation is compared with the duration of the pulse train. Expecting that the generation of negative pressures will be the result of radial wave reflection, an analysis was carried out by focusing on the jet cross-section with peak energy deposition. Figure 4 depicts various snap shots of the pressure profile during radial wave propagation and reflection. Following the initial pressure distribution (at the end of the 2-ns pulse) a pressure waves initiate due to gradients and traverse the jet radius. As seen from the analysis results excessive negative pressures (above 50 MPa) appear after more than 2.2 μs have elapsed. Such time is larger than the time needed for all six 2-ns pulses to be delivered.

Figure 5 depicts the pressure oscillations in the jet and at several radial distances. Of importance is the first half-cycle which indicates that the jet is in positive pressure state throughout for the time of interest.
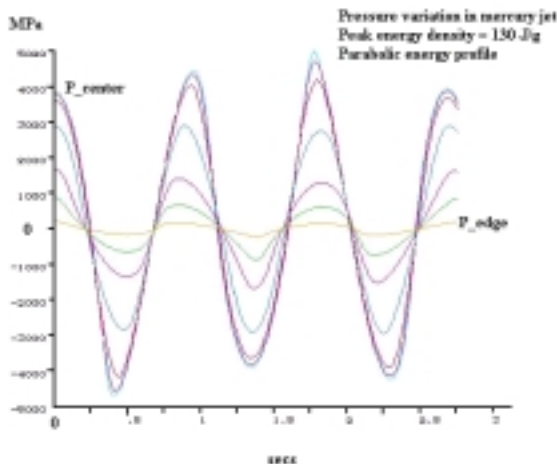

Figure 5: Pressure radial oscillations in mercury jet

2.6 Pressure Wave-Jet Nozzle Interaction

The initial pressures that are generated in the interaction zone of the jet are approaching 3800 MPa. While the interaction zone of the jet may be broken up a few microseconds after the proton beam arrival, the upstream section of the jet is still intact and will allow for the propagation of pressure waves toward the nozzle. At issue is the amplitude of the pressure wave front when it arrives at the nozzle and impacts on the walls. The estimated time of the arrival of the front is

approximately 100 μs based on a 15-cm distance between the beginning of the interaction zone and the nozzle. Figure 1 shows the schematic of the model that was used.

Figures 6-8 show snapshots of the pressure profile along the mercury jet in a cut through the long axis. While pressures start out as positive as a result of the rapid energy deposition and the inability of the Hg to accommodate the thermal expansion, it quickly turns negative in the center of the interaction zone as a result of the wave reflections and sign reversal from the free surface of the jet. While part of the interaction region may be destroyed, the pressure front will advance toward the nozzle through the undisturbed jet.
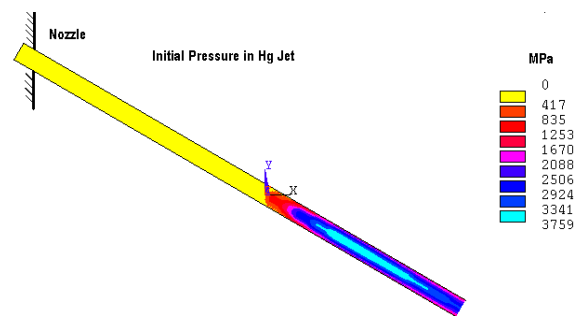

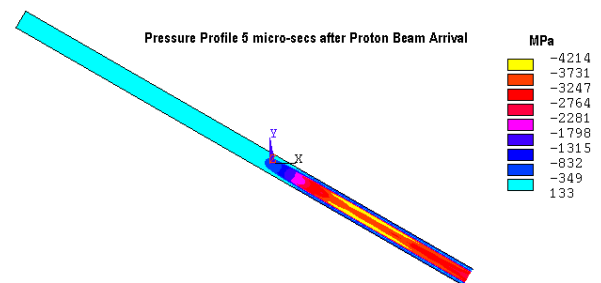
Figure 6: Initial Pressure in the Hg Jet

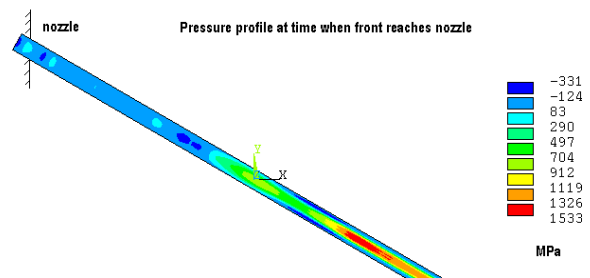**Figure 7: Pressure profile at 5 μs after beam arrival**

Figure 8: Pressure profile upon arrival of the front at nozzle location

As expected, the pressure wave will attenuate as it travels through the undisturbed part of the jet. Figure 9 depict the pressure wave fluctuation and amplitude at different in the nozzle vicinity. The amplitude of the pressure wave when it arrives at the nozzle is approximately 100 MPa. While such a pressure may result in nozzle and jet channel stresses that are below the strength limits, a large number of such impacts will accumulate during the operation of the machine that may lead to fatigue failure. The latter becomes more of an issue considering the high irradiation doses the structural materials will receive because of their proximity to the target.
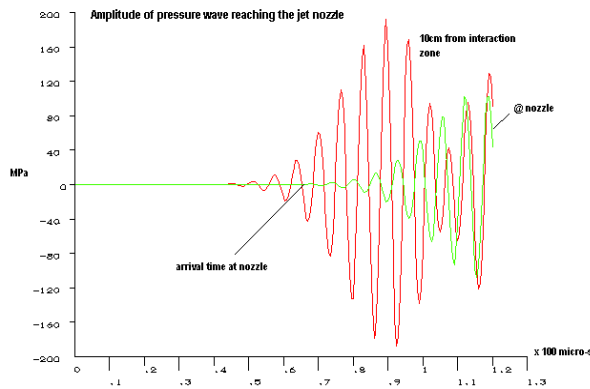

Figure 9: Pressure wave amplitude arriving at nozzle

3. EXPERIMENTAL RESULTS
BNL E951

In the BNL muon targetry experiment E951 the interaction of a mercury jet with a proton beam was studied without the 20 Tesla magnetic field. A schematic of the target chamber is shown in Figure 10.
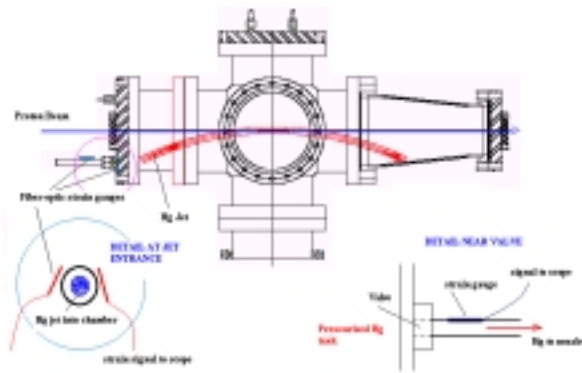

Figure 10: Schematic of the BNL E951 set-up for the mercury jet target test including the strain gauge array

To record the mercury jet dispersal two camera systems were used with recording capabilities: 1) at rate of 4 kHz with shutter settings for each frame set to 25 μs and 2) 16 frames at speeds up to 1 MHz and exposure time of 150 ns per frame.

The potential pressure wave effect on the jet nozzle was recorded with the use of fiber-optic strain gauges that were placed on the jet target enclosure as shown in Figure 10.

3.1 Mercury Jet Experimental Results

In the E951 experiment the mercury jet trajectory overlapped with the proton beam for 19 cm. The diameter of the jet at the interaction region ranged between 0.7 cm and 1.7 cm. Achieved proton beam intensities ranged between 0.5-4.0 TP and spot sizes were of the order of 1.6 mm in x-dir and 0.9 mm in y-dir rms sigma radius.

Dispersal of the mercury was observed by viewing prominences as they left the bulk of the mercury jet. Figure 11 depicts a series of frames recorded during the experiment showing the evolution of the jet dispersion. Of importance is the time scales in which events occur. Specifically, the appearance of material emanating from the free jet surface occurs at 0.75 ms. However, a fast camera with capabilities of 1 frame/μs revealed that the initiation of jet dispersion occurred at a time of ~ 40μs. Such delay time from the onset of proton beam/jet interaction is well in line with the estimates made on the basis of volumetric expansion within the jet. Further, measured velocities of 5 to 50 m/s also tend to agree with velocities estimated from $U_r = \sqrt{2} [\alpha_v \Delta T] c$ in which, as observed, the bulk velocity of ejected material is proportional to the temperature rise, which in turn is directly proportional to the intensity of the impinging protons.
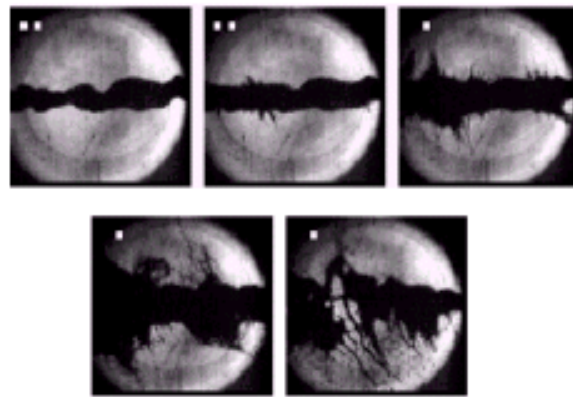

Figure 11: Mercury jet interaction with 24 GeV 3.8 TP beam of the E951 experiment; t = 0 ms; .75 ms; 2 ms; 10 ms; 18 ms

3.2 Jet Nozzle Results

The available set-up provided an opportunity to address the issue of shock waves reaching the jet nozzle. As a result, four fiber optic strain gauges were placed at selected locations in the mercury line (shown in Figure 10). Specifically, a gauge was placed on the line that supplies mercury to the jet just upstream of the nozzle. This gauge, placed along the pipe as shown, is expected to register any activity associated with a wave returning from the jet. The geometry and size of the supply pipe did not allow for the gauge to be placed with hoop orientation. Potential strains along the hoop direction in the pipe wall are expected to be much higher than the axial and thus more easily detectable. Strains in the supply pipe will be the direct result of the pressure in the contained mercury.

In addition to the nozzle gauge, one was placed at the valve outlet (furthest location in the supply pipe upstream of the nozzle) and two were installed on the nozzle mounting plate on either side of the nozzle. Strains for beam intensities ranging between 0 TP and 4 TP (0 TP being the case of jet activity alone) were recorded. While the beam intensity was much lower than anticipated, thus keeping the potential strain aggravation due to shock quite low, still some clear evidence of activity was recorded. Shown in Figure 12 is the strain recorded by the nozzle gauge for back-to-back pulses with similar intensities (3.75 TP). The stability in the measuring system is shown to be excellent. The front part of the record is the noise from the flowing Hg in the supply pipe. The spike indicates the arrival of the proton beam and it is the effect of photons on the gauges. Beyond that there is clear evidence of activity induced by the proton beam interacting with the jet. Figure 13 quantifies the effect by comparing the strain induced by the jet alone with that of the interaction.
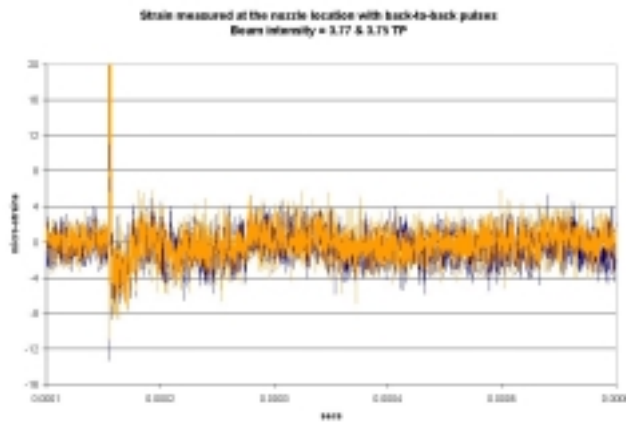

Figure 12: Strain near nozzle from back-to-back proton pulses of same intensity
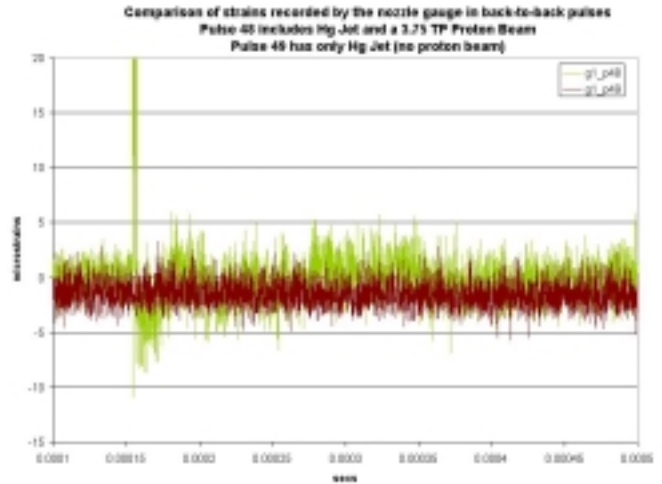

Figure 13. Strain comparison between the case of (a) jet and beam interaction and (b) jet only

4. SUMMARY

Based on (a) theoretical/computational predictions of the behavior of a mercury jet interacting with an energetic, focused proton beam and (b) on observations made during the E951 experiment the following conclusions are made:

- Thermodynamic analysis of the interaction process shows that for a train of six, 2-ns long micro-pulses brought on target within 2 μs the target has a chance of survival (not dispersing) in the new titled configuration. In the head-on interaction, however, parts of the jet interaction region will exceed the critical state and the post jet behavior is hard to predict.

- Generated pressure waves induce high negative stresses that try to break the jet apart but their on-set is slightly longer than the 2 μs time span assumed for beam delivery.

- Dispersion of the jet, as predicted and also verified by the E951 experiment, is a much longer process than sound travelling. Further, the predicted velocities of the ejected material from the jet were generally confirmed.

- Evidence of pressure waves travelling back toward the nozzle was seen in the E951 experiment. The achieved beam intensities, however, were not high enough such that definitive statements about the survivability of the nozzle can be made.

ACKNOWLEDGMENTS

REFERENCES

[1] S. Osaki et al., eds., "Feasibility Study-II of a Muon Based Neutrino Source," http://www.cap.bnl.gov/mumu/studyii/FS2-report-html

[2] N.Simos et al., "Thermodynamic Interaction of the Primary Proton Beam with a Mercury Jet Target at a Neutrino Factory Source," PAC2001, RPAH076.

[3] H. Kirk et al, "Target Studies with BNL E951 at the AGS," PAC2001, TPAH137.

[4] A. Hassanein and I. Konkashbaev, "Thermoelastic Response of Suddenly Heated Liquid and Solid Targets for High Power Colliders," PAC2001, RPAH071.

[5] P. Thieberger, "Estimated perturbations of the Axial motion of a liquid-metal jet entering a strong magnetic field," http://www-mucool.fnal.gov/ mcnotes/muc0182.pdf.

[6] K.T. McDonald, "Magneto-hydrodynamics of a Continuous Mercury Jet Coaxially Entering a Solenoid," http://puhep1.princeton.edu/mumu/target/continuousjets.ps.

[7] S. Kahn et al., "Calculations for Mercury Jet Target in a Solenoid Magnet Capture System," PAC2001, ROPB010.

[8] P. Sivers and P. Pugnat, " Response of Solid and Liquid Targets to High Power Proton Beams for Neutrino Factories," CERN-NuFACT Note 035.

[9] SESAME Library, SANL.

[10] V. W. Sonntag, "Fundamentals of Classical Thermodynamics", 2nd Edition, Wiley, 1973.

[11] N.V. Mokhov, "The MARS Code System User Guide, Version 13 (95)", 1995.

[12] N. Molkov, Private communication.

[13] ANSYS Engineering Analysis of Systems, Swanson Analysis Systems Inc., 1999.